Kinetics and Mechanisms of the Gas-Phase Reactions of the NO_3 Radical with Aromatic Compounds

ERIC S. C. KWOK[†], ROGER ATKINSON[*,‡], and JANET AREY[*,‡]
Statewide Air Pollution Research Center, University of California, Riverside, California 92521

Abstract

The kinetics and nitrated products of the gas-phase reactions of the NO_3 radical with methoxybenzene, 1,2-, 1,3-, and 1,4-dimethoxybenzene, dibenzofuran and dibenzo-*p*-dioxin have been investigated at 297 ± 2 K and in the presence of one atmosphere of air. A relative rate method was used for the kinetic measurements. No reactions of methoxybenzene or dibenzofuran with the NO_3 radical were observed. The dimethoxybenzenes were observed to react by H-atom abstraction and NO_3 radical addition to the aromatic ring, while dibenzo-*p*-dioxin reacted by NO_3 radical addition to the aromatic rings. For these compounds, the NO_3 radical addition pathways were observed to be reversible. At the NO_2 concentrations employed, the NO_3-aromatic adducts reacted with NO_2 and the observed rate constants increased with increasing NO_2 concentration. However, for dibenzo-*p*-dioxin the observed rate constant became independent of the NO_2 concentration for concentrations $\gtrsim 4.8 \times 10^{13}$ molecule cm^{-3}, and under these conditions the rate constant of 6.8×10^{-14} cm^3 molecule^{-1} s^{-1} was taken to be that for addition of the NO_3 radical to the aromatic rings. The proposed NO_3 radical reaction mechanisms are discussed.

Introduction

The gas-phase reactions of the NO_3 radical with aromatic compounds have been shown [1–6] to proceed by two pathways: H-atom abstraction from, or NO_3 radical addition to, the substituent groups [1,2,4–6], and reversible NO_3 radical addition to the aromatic ring, with the NO_3-aromatic adduct undergoing thermal decomposition back to reactants or reacting with NO_2 to form products [1,3,4]. For example, for toluene the reaction proceeds by H-atom abstraction from the $-CH_3$ substituent group [1,4] to form the benzyl radical, and similarly for other alkyl-substituted benzenes [1,4,5]. The NO_3 radical reactions with styrene and acenaphthylene proceed by NO_3 radical addition to the $\rangle C{=}C\langle$ bond of the substituent group (styrene) or the unsaturated penta-fused ring (acenaphthylene) [1,2,4,6], to form a thermally stable nitrato-alkyl radical which then reacts with O_2, with the reaction sequence being analogous to those for the NO_3 radical reactions with the alkenes [4,7].

However, for naphthalene the NO_3 radical reaction has been shown to proceed by initial addition of the NO_3 radical to the aromatic ring, followed by either decomposition of the NO_3-aromatic adduct back to reactants or reaction with NO_2 to form products, including nitronaphthalenes [3,4].

---

[*] To whom correspondence should be addressed.

[†] Interdepartmental Graduate Environmental Toxicology Program, University of California, Riverside, California 92521.

[‡] Also, Department of Soil and Environmental Sciences, University of California, Riverside, California 92521.

International Journal of Chemical Kinetics, Vol. 26, 511–525 (1994)
CCC 0538-8066/94/050511-15

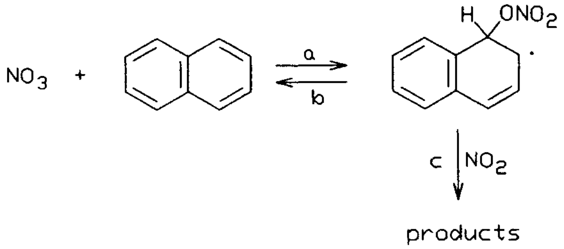

Scheme I

With this reaction scheme, the measured rate constant k_{obs} is given by

$$k_{obs} = k_a k_c[NO_2]/(k_b + k_c[NO_2]) \tag{I}$$

where k_a, k_b, and k_c are the rate constants for reactions (a), (b), and (c), respectively. Under conditions that $k_b >> k_c[NO_2]$, then $k_{obs} = k_a k_c[NO_2]/k_b$ and the measured rate constant depends linearly on the NO_2 concentration. Since under the experimental conditions generally employed in previous kinetic studies [1,8–10], NO_3 radicals, NO_2 and N_2O_5 were at, or close to, equilibrium,

$$NO_2 + NO_3 \overset{M}{\rightleftharpoons} N_2O_5$$

then the reactions in NO_3—NO_2—N_2O_5-air mixtures appeared to be kinetically equivalent to reaction with N_2O_5. This behavior has been observed for naphthalene [1,4,8,9], naphthalene-d_8 [4,11], 1- and 2-methylnaphthalene [1,4,10] and 2,3-dimethylnaphthalene [1,4,10]. For acenaphthene, the NO_3 radical reaction proceeds by both H-atom abstraction from the —CH_2— groups and reversible NO_3 radical addition to the aromatic rings [1,2,4]. For acenaphthene, as for other aromatic compounds which react by both H-atom abstraction from the substituent group and reversible NO_3 radical addition to the aromatic ring(s), Eq. (I) must be modified to

$$k_{obs} = k_{abs} + k_a k_c[NO_2]/(k_b + k_c[NO_2]) \tag{II}$$

where k_{abs} is the rate constant for the H-atom abstraction pathway [1].

The experimental data of Atkinson et al. [3] for naphthalene, when combined with either estimates of the rate constants for reactions (a) and (c) from the analogous OH radical addition to aromatic hydrocarbons [12] or with the thermochemistries of OH radical addition to benzene and naphthalene [4,12], allow a rate constant for the thermal decomposition of the NO_3-naphthalene adduct at 298 K and atmospheric pressure of air of ca. 7×10^5 s^{-1} to be obtained [4]. A thermal decomposition rate constant for the NO_3-benzene adduct at 298 K of ca. 5×10^8 s^{-1} has also been calculated [4], a factor of ca. 10^3 higher than that for the NO_3-naphthalene adduct and consistent with the observed lack of reaction of benzene with the NO_3 radical [4]. Based on these limited data, it is then expected that the overall NO_3 radical addition to monocyclic aromatic ring systems, via reactions (a), (b), and (c), will be markedly slower than the NO_3 radical addition to fused-ring polycyclic aromatic ring systems [4].

It may therefore be expected that dibenzo-*p*-dioxin and dibenzofuran would behave like benzene and biphenyl [4]. However, during a study of the atmospheric chemistry of dibenzo-*p*-dioxin and dibenzofuran [13], we observed that dibenzo-*p*-dioxin reacts relatively rapidly with the NO_3 radical. We report here the results of kinetic studies of the gas-phase reactions of the NO_3 radical with dibenzo-*p*-dioxin and dibenzofuran and with the structurally related compounds, methoxybenzene and 1,2-, 1,3-, and 1,4-dimethoxybenzene.

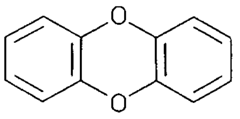

Dibenzo-p-dioxin

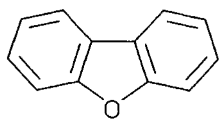

Dibenzofuran

To aid in the interpretation of the reaction pathways operating, the nitro-products of these reactions were also identified and quantified.

Experimental

All experiments were carried out in the dark in 6400–6900 liter all-Teflon chambers at 297 ± 2 K and in the presence of ca. 735 torr total pressure of dry (relative humidity ca. 3–5%) pure air.

Kinetic Studies

The experimental procedures used were generally similar to those described previously [1,14,15]. A relative rate method was used in which the relative disappearance rates of the aromatic compound and the reference alkene, 1-butene, were monitored in the presence of NO_3 radicals [1,14,15]. NO_3 radicals were generated by the thermal decomposition of N_2O_5.

$$N_2O_5 \xrightarrow{M} NO_3 + NO_2$$

NO_2 was generally added to the reactant mixtures to investigate the effect of the NO_2 concentration on the measured NO_3 radical reaction rate constant k_{obs}, and also served to scavenge any OH radicals produced in these reactions [15]. As discussed below, NO_2 was not added to the reactant mixtures for certain experiments with dibenzo-*p*-dioxin, and in these experiments a large excess concentration of ethane was added to scavenge any OH radicals formed [1,15]. Providing that the aromatic compound and 1-butene reacted only with the NO_3 radical, then

$$\text{(III)} \qquad \ln\left\{\frac{[\text{aromatic}]_{t_0}}{[\text{aromatic}]_t}\right\} - D_t = \frac{k_{obs}}{k_2}\left[\ln\left\{\frac{[\text{1-butene}]_{t_0}}{[\text{1-butene}]_t}\right\} - D_t\right]$$

where $[\text{aromatic}]_{t_0}$ and $[\text{1-butene}]_{t_0}$ are the concentrations of the aromatic compound and 1-butene at time t_o, respectively, $[\text{aromatic}]_t$ and $[\text{1-butene}]_t$ are the corresponding concentrations at time t, D_t is the amount of dilution caused by successive additions of N_2O_5 to the chamber during an experiment ($D_t = 0.0014$ per N_2O_5 addition), and k_{obs} and k_2 are the rate constants for reactions (1) and (2), respectively.

$$\text{(1)} \qquad NO_3 + \text{aromatic compound} \longrightarrow \text{products}$$

$$\text{(2)} \qquad NO_3 + \text{1-butene} \longrightarrow \text{products}$$

While the rate constant for reaction (2) is independent of the NO_2 concentration [4,7], the observed rate constant for reaction (1), k_{obs}, may increase with the NO_2 concentration. Hence, at least for a constant NO_2 concentration, a plot of $\{\ln([\text{aromatic}]_{t_0}/[\text{aromatic}]_t) - D_t\}$ against $\{\ln([\text{1-butene}]_{t_0}/[\text{1-butene}]_t) - D_t\}$ should be a straight line with zero intercept.

The initial reactant concentrations were (in molecule cm^{-3} units): dibenzo-*p*-dioxin, (1.6–3.4) × 10^{11}, dibenzofuran, (6.5–8.1) × 10^{11}, methoxybenzene, 7.4 × 10^{12}, 1,2-dimethoxybenzene, (7.9–8.9) × 10^{12}, 1,3-dimethoxybenzene, (4.2–8.1) × 10^{12}, and 1,4-dimethoxybenzene, (0.79–1.02) × 10^{13}; 1-butene, ca. 4.8 × 10^{13}; NO_2 (when present), (4.8–120) × 10^{13} or ethane, 2.4 × 10^{16}; and 3 to 5 additions of N_2O_5 (corresponding to initial N_2O_5 concentrations in the chamber of (0.6–9.9) × 10^{13} molecule cm^{-3} per addition) were made to the chamber during an experiment. The concentrations of the aromatic compound and 1-butene were measured by gas chromatography with flame ionization detection (GC-FID) during the experiments. For the analyses of 1-butene, gas samples were collected from the chamber in all-glass, gas-tight syringes and transferred via a 1 cm^3 loop and gas sampling valve onto a 30 m DB-5 megabore column held at −25°C and then temperature programmed at 8°C min^{-1}. For the analyses of dibenzo-*p*-dioxin, dibenzofuran, methoxybenzene, and the dimethoxybenzenes, gas samples of 100 cm^3 volume (for methoxybenzene and the dimethoxybenzenes) or 460–1150 cm^3 volume (for dibenzofuran and dibenzo-*p*-dioxin) were collected from the chamber onto Tenax-TA solid adsorbent, with subsequent thermal desorption at 250°C onto a 15 m DB-5 megabore column held at 40°C and then temperature programmed at 10°C min^{-1}. The initial NO_2 concentrations were calculated from the amounts of NO_2 introduced into the chamber.

Nitroaromatic Product Formation

The nitro-products of these NO_3 radical reactions were identified and their formation yields determined from samples collected during, or after, the kinetic experiments. For the dimethoxybenzene isomers, gas samples were collected onto Tenax-TA solid adsorbent with subsequent thermal desorption and analysis by combined gas chromatography-mass spectrometry (GC/MS), using a Hewlett Packard (HP) 5890 GC with a 60 m DB-5 capillary column temperature programmed from −25°C at 8°C min^{-1}, interfaced to an HP 5971 mass selective detector. GC-FTIR analyses were also conducted by thermal desorption of samples collected onto Tenax solid adsorbent using an HP 5890 GC with a 25 m HP-5 column (0.32 μm diameter, thick film), temperature programmed from −25°C at 8°C min^{-1}, interfaced to an HP 5965B FTIR detector. Identification of the nitrodimethoxybenzenes was confirmed by matching their GC retention times, mass spectra, and IR spectra with those of authentic standards. Nitrodimethoxybenzene formation was sufficient that these products could be quantified by GC-FID with the same samples used to monitor the parent dimethoxybenzenes during the kinetic experiments.

Because of the low initial concentrations of dibenzo-*p*-dioxin necessitated by the low vapor pressure of dibenzo-*p*-dioxin of ca. 4 × 10^{-4} torr at 298 K [16], nitrodibenzo-*p*-dioxins were analyzed using ca. 2000 liter volume gas samples collected from the chamber at the end of the NO_3 radical reactions onto two polyurethane foam (PUF) plugs in series. The PUF plugs were solvent extracted by CH_2Cl_2 for 4 hr using a Soxhlet extractor and fractionated by high performance liquid chromatography (HPLC) using a HP 1040 with diode array detector. The solvent program (at a flow rate of 3 ml min^{-1}) was: initially 100% hexane for 10 min, followed by a 5 min linear gradient to 95% hexane/5% CH_2Cl_2, then programmed over the next 25 min to 100% CH_2Cl_2 where it was held for 10 min, then programmed to 100% acetonitrile over a 10 min period, held isocratic for 10 min, and then programmed back to the initial conditions. The HPLC fractions were analyzed by GC/MS using the same instrumentation described above, and the nitrodibenzo-*p*-dioxin identified by comparing the GC retention time and mass spectrum with those of a synthesized standard. Quantification was carried out by GC/MS using 2-nitrofluorene as an internal standard.

Chemicals

The sources of the chemicals used, and their stated purities, were: dibenzofuran (99+%), 1,2-dimethoxybenzene (99%), 1,3-dimethoxybenzene (99%), 1,4-dimethoxybenzene (99%), methoxybenzene (99%), and 4-nitro-1,2-dimethoxybenzene (99%), Aldrich Chemical Company; dibenzo-*p*-dioxin (99%), AccuStandard; 4-nitro-1,3-dimethoxybenzene (99%), ICN; 2-nitro-1,4-dimethoxybenzene, American Tokyo Kasei; and 1-butene (99%) and NO (≥99.0%), Matheson Gas Products. NO_2 was prepared prior to use by reacting NO with an excess of O_2. 2-Nitrodibenzo-*p*-dioxin was synthesized by reacting dibenzo-*p*-dioxin with nitric acid as described by Saint-Ruf and Lobert [17], and its identity confirmed by ^{1}H NMR.

Results

Kinetics

The relative disappearance rates of the aromatic compounds and 1-butene were monitored in N_2O_5—NO_3—NO_2-aromatic-1-butene-air mixtures. Within the analytical uncertainties, no reactions of methoxybenzene or dibenzofuran in these reactant mixtures were observed, as shown, for example, from the plot of eq. (III) for dibenzofuran in Figure 1. From the amounts of 1-butene reacted and assuming <10% reaction of methoxybenzene and dibenzofuran, then the upper limits to the rate constants ratios k_{obs}/k_2 given in Table I are obtained. In contrast, dibenzo-*p*-dioxin and the dimethoxybenzenes were observed to react in the presence of NO_3 radicals, and plots of eq. (III) at various initial NO_2 concentrations for dibenzo-*p*-dioxin and 1,2-dimethoxybenzene are shown in Figures 1 and 2, respectively. The slopes of these plots, k_{obs}/k_2, at the various initial NO_2 concentrations employed are also given in Table I.

For all three of the dimethoxybenzenes, the slopes of the plots of eq. (III), k_{obs}/k_2, increased with increasing initial NO_2 concentration (Table I), as shown in Figure 2 for 1,2-dimethoxybenzene. Plots of these slopes, k_{obs}/k_2, against the NO_2 concentrations are shown in Figure 3. Reasonably good straight line plots are seen, with the nonzero intercepts suggesting that the NO_3 radical reactions proceed by H-atom abstraction from the —OCH_3 groups as well as by reversible NO_3 radical addition to the aromatic ring, as described by eq. (II). The least-squares slopes, $k_a k_c/k_b k_2$, and intercepts, k_{abs}/k_2, of the plots shown in Figure 3 are given in Table II.

The experimental data obtained for dibenzo-*p*-dioxin in the presence of initially added NO_2 (Figure 1) show that within the experimental uncertainties the observed rate constant is independent of the initial NO_2 concentration over the range $(4.8-24) \times 10^{13}$ molecule cm^{-3}. These data are consistent with either a direct, NO_2 concentration-independent, reaction or with reversible NO_3 radical addition to the aromatic rings (Reaction Scheme I) with $k_c[NO_2] >> k_b$ for $[NO_2] \geq 4.8 \times 10^{13}$ molecule cm^{-3}. These two possibilities were investigated by conducting experiments with no initially present NO_2, but with 2.4×10^{16} molecule cm^{-3} of ethane present to

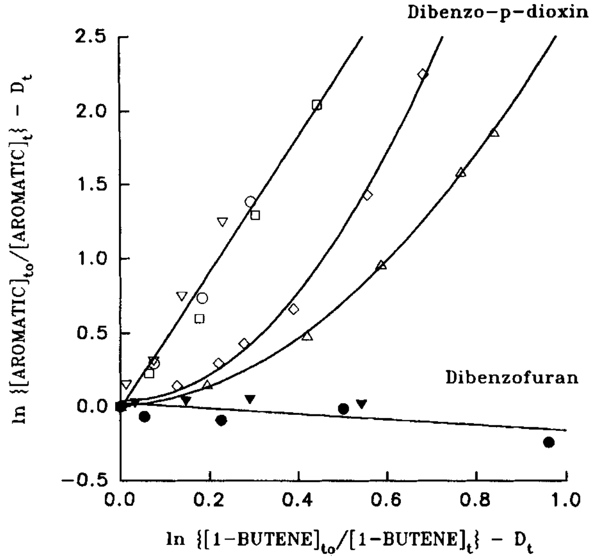

Figure 1. Plots of eq. (III) for the gas-phase reactions of the NO_3 radical with dibenzofuran and dibenzo-*p*-dioxin, with 1-butene as the reference alkene. Initial NO_2 concentrations (molecule cm^{-3}): (△, ◇) no initially added NO_2, but with 2.4×10^{16} molecule cm^{-3} of ethane; (□) 4.8×10^{13}; (○,●) 1.2×10^{14}; and (▽,▼) 2.4×10^{14}.

scavenge any OH radicals formed in the NO_3 radical reaction systems [1,15]. In these reactions, the NO_2 concentrations were initially low but were expected to increase with the extent of reaction due to formation of NO_2 during the reactions from the thermal decomposition of N_2O_5. Hence, if the reaction scheme involves only reactions (a), (b),

TABLE I. Rate constant ratios k_{obs}/k_2 for the gas-phase reactions of the NO_3 radical with selected aromatic compounds at 297 ± 2 K.

Aromatic	$10^{-13} \times [NO_2]$ (molecule cm^{-3})	k_{obs}/k_2 [a]
Methoxybenzene	4.8–24	<0.1
1,2-Dimethoxybenzene	4.8	1.10 ± 0.16
	12	2.11 ± 0.18
	24	2.73 ± 0.28
	48	4.96 ± 0.28
1,3-Dimethoxybenzene	4.8	0.791 ± 0.174
	24	1.68 ± 0.31
	24	1.77 ± 0.33
	48	2.13 ± 0.10
	48	1.92 ± 0.13
	120	4.18 ± 0.33
1,4-Dimethoxybenzene	4.8	1.27 ± 0.16
	24	3.53 ± 0.65
	48	6.15 ± 1.66
Dibenzofuran	12–24	<0.1
Dibenzo-*p*-dioxin	4.8	4.62 ± 0.57
	12	4.70 ± 0.70
	24	5.31 ± 0.73

[a] Indicated errors are two least-squares standard deviations.

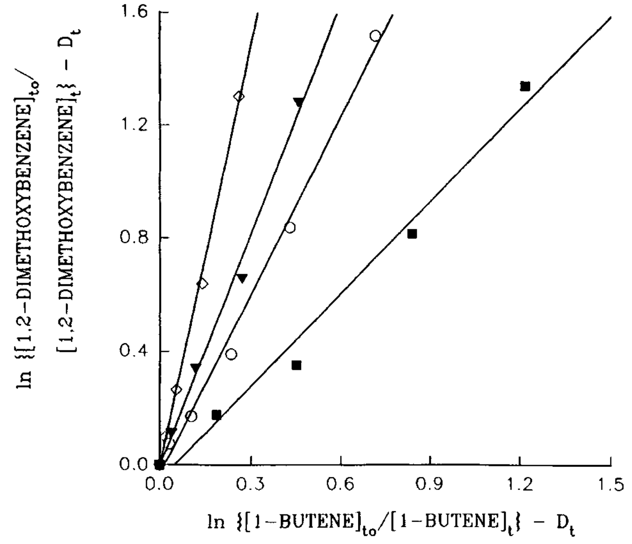

Figure 2. Plots of eq. (III) for the gas-phase reactions of the NO_3 radical with 1,2-dimethoxybenzene, with 1-butene as the reference alkene. Initial NO_2 concentrations (molecule cm^{-3}) were: (■) 4.8 × 10^{13}; (○) 1.2 × 10^{14}; (▼) 2.4 × 10^{14}; and (◇) 4.8 × 10^{14}.

and (c), then a plot of eq. (III) will be curved, with the slope increasing with increasing extent of reaction of the 1-butene and aromatic compound [1,8]. Such curved plots were observed, as shown in Figure 1, with the slope of the plots increasing from close to zero to values reasonably similar to those obtained from the experiments conducted with initial NO_2 concentrations of (4.8–24) × 10^{13} molecule cm^{-3} (Fig. 1).

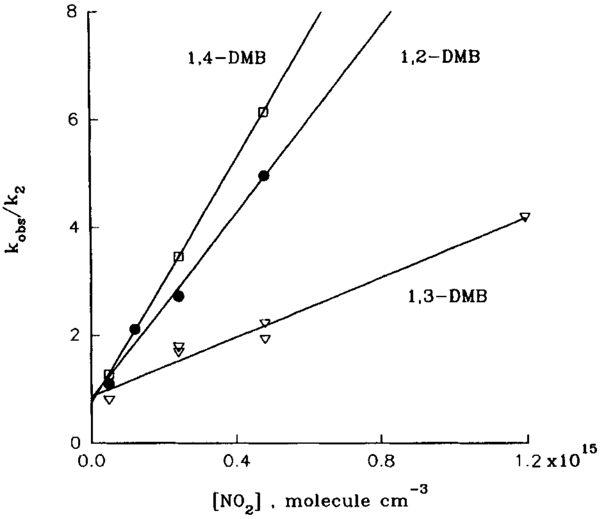

Figure 3. Plots of k_{obs}/k_2 against the initial NO_2 concentration for the gas-phase reactions of the NO_3 radical with 1,2-, 1,3-, and 1,4-dimethoxybenzene (DMB), where k_2 is the rate constant for the NO_3 radical reaction with 1-butene.

TABLE II. Rate constants ratios $k_{abs}/k_2, k_a k_c/k_b k_2, k_a k_c/k_b, k_b/k_c$, and rate constants k_{abs} and k_a for the gas-phase reactions of the NO_3 radical with a series of aromatic compounds at 297 ± 2 K.

Aromatic	k_{abs}/k_2 [a]	$10^{15} \times k_a k_c/k_b k_2$ [a] (cm^3 $molecule^{-1}$)	k_{abs} [b] (cm^3 $molecule^{-1}$ s^{-1})	$k_a k_c/k_b$ [b] (cm^6 $molecule^{-2}$ s^{-1})
Methoxybenzene	<0.1	<0.42	$<1.6 \times 10^{-15}$	$<7 \times 10^{-30}$
1,2-Dimethoxybenzene	0.82 ± 0.40	8.6 ± 1.5	$(9.8 \pm 5.7) \times 10^{-15}$	$(1.0 \pm 0.4) \times 10^{-28}$
1,3-Dimethoxybenzene	0.86 ± 0.29	2.8 ± 0.5	$(1.02 \pm 0.47) \times 10^{-14}$	$(3.3 \pm 1.2) \times 10^{-29}$
1,4-Dimethoxybenzene	0.74 ± 0.05	11.3 ± 0.2	$(8.8 \pm 2.8) \times 10^{-15}$	$(1.3 \pm 0.4) \times 10^{-28}$
Dibenzofuran	<0.1	<0.42	$<1.6 \times 10^{-15}$	$<7 \times 10^{-30}$
Dibenzo-*p*-dioxin	<0.5		$<8 \times 10^{-15}$	3.9×10^{-27} [c]

[a] Indicated errors are two least-squares standard deviations.

[b] Placed on an absolute basis by use of a rate constant for the reaction of the NO_3 radical with 1-butene of $k_2 = 1.19 \times 10^{-14}$ cm^3 $molecule^{-1}$ s^{-1} (±30%) at 297 K [7]. Indicated errors are two least-squares standard deviations combined with the estimated overall uncertainties in k_2.

[c] Uncertain by a factor of ca. 2; see text.

Nitro-products

GC/MS and GC-FTIR analyses of the reacting mixtures showed the formation of 4-nitro-1,2-dimethoxybenzene from 1,2-dimethoxybenzene, 4-nitro-1,3-dimethoxybenzene from 1,3-dimethoxybenzene, and 2-nitro-1,4-dimethoxybenzene from 1,4-dimethoxybenzene. In several of the experiments, plots of the amounts of the nitrodimethoxybenzene against the amounts of dimethoxybenzene reacted exhibited marked curvature, with the apparent yield generally decreasing with increasing extent of reaction (Fig. 4). The degree of curvature in these plots was somewhat random, and could be due to secondary reactions of the nitrodimethoxybenzenes with the NO_3 radical or losses to the chamber walls. Since 2-nitrophenol and the nitronaphthalenes have been shown to be less reactive than phenol and naphthalene, respectively, towards reaction with the NO_3 radical [4,18,19], it may be anticipated that the nitrodimethoxybenzenes would also be less reactive than the parent dimethoxybenzenes. The estimated vapor pressures of 2-nitro-1,4-dimethoxybenzene and 4-nitro-1,2-dimethoxybenzene are ca. $(2.5-4.5) \times 10^{-4}$ torr at 298 K, based on their boiling points and assuming a similar slope of the ln(vapor pressure) vs. T^{-1} curve as for 1,2-dimethyl-4-nitrobenzene [20]. This magnitude of vapor pressure suggests that wall losses are the likely explanation for the observation of decreasing nitrodimethoxybenzene yields with extent (or time) of reaction. Accordingly, the nitrodimethoxybenzene formation yields were derived from the initial data points, and these formation yields are given in Table III.

GC/MS analyses of the HPLC-separated fractions of the extracts of the samples collected on PUF plugs from reacted N_2O_5—NO_3—NO_2-dibenzo-*p*-dioxin-air mixtures showed the presence of only one of the two possible nitrodibenzo-*p*-dioxins. Comparison with the GC retention time and mass spectrum of the synthesized standard of 2-nitrodibenzo-*p*-dioxin showed that the nitro-product from the NO_3 radical-initiated reaction of dibenzo-*p*-dioxin was 2-nitrodibenzo-*p*-dioxin. The formation yield obtained from GC/MS analyses is given in Table III.

Discussion

The rate constant ratios k_{abs}/k_2 and $k_a k_c/k_b k_2$ can be placed on an absolute ba-

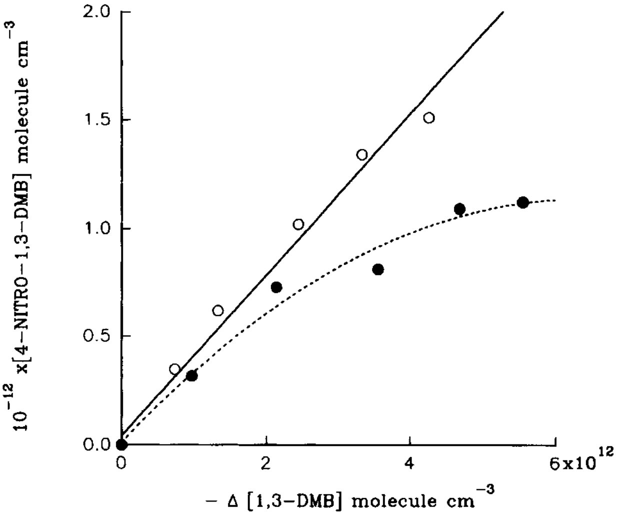

Figure 4. Plots of the amounts of 4-nitro-1,3-dimethoxybenzene formed against the amount of 1,3-dimethoxybenzene (1,3-DMB) reacted with the NO_3 radical for two experiments with the same initial NO_2 concentration of 1.2×10^{15} molecule cm^{-3}.

sis by using a rate constant for the reaction of the NO_3 radical with 1-butene of $k_2 = 1.19 \times 10^{-14}$ cm^3 molecule^{-1} s^{-1} (±30%) at 297 K [7], and the resulting rate constants k_{abs} and $k_a k_c/k_b$ are given in Table II. For the aromatic compounds studied here, literature data are available only for methoxybenzene [4,21,22], and the upper limit to the rate constant of $k_{abs} < 1.6 \times 10^{-15}$ cm^3 molecule^{-1} s^{-1} obtained here is

TABLE III. Measured nitro-product formation yields from the gas-phase reactions of the NO_3 radical with the dimethoxybenzenes and dibenzo-*p*-dioxin.

Aromatic	$10^{-13} \times [NO_2]$ molecule cm^{-3}	Product	Yield[a] Observed	Yield[a] From NO_3 addition
1,2-Dimethoxybenzene	4.8	4-Nitro-1,2-dimethoxybenzene	0.137 ± 0.039	0.41 ± 0.12
	48		0.484 ± 0.049	0.58 ± 0.06
1,3-Dimethoxybenzene	4.8	4-Nitro-1,3-dimethoxybenzene	0.048 ± 0.027	0.36 ± 0.21
	24		0.147 ± 0.001	0.34 ± 0.01
	24		0.224 ± 0.069	0.51 ± 0.16
	48		0.349 ± 0.107	0.58 ± 0.18
	48		0.137 ± 0.013	0.23 ± 0.03
	120		0.341 ± 0.013	0.43 ± 0.02
	120		0.416 ± 0.044	0.52 ± 0.06
1,4-Dimethoxybenzene	4.8	2-Nitro-1,4-dimethoxybenzene	0.117 ± 0.026	0.28 ± 0.07
	24		0.088 ± 0.056	0.11 ± 0.08
	48		0.192 ± 0.064	0.22 ± 0.08
Dibenzo-*p*-dioxin	24	2-Nitrodibenzo-*p*-dioxin	0.002	0.002

[a] Indicated errors are two least-squares standard deviations and do not include the uncertainties in the GC-FID calibration factors for the reactants and nitro-products.

consistent with the rate constants previously determined by Atkinson et al. [22] of (1–2) × 10^{-16} cm^3 $molecule^{-1}$ s^{-1} at 294 K [4,22].

The measured nitrodimethoxybenzene product formation yields from the NO_3 radical reactions with the dimethoxybenzenes (Table III) show a general increase in yield with increasing NO_2 concentration. This observation is consistent with the kinetic data which indicate that the NO_3 radical addition path to the aromatic ring increases with increasing NO_2 concentration. Thus, the NO_3 radical reactions with the dimethoxybenzenes proceed by two pathways: H-atom abstraction from the —OCH_3 groups and NO_3 radical addition to the aromatic rings,

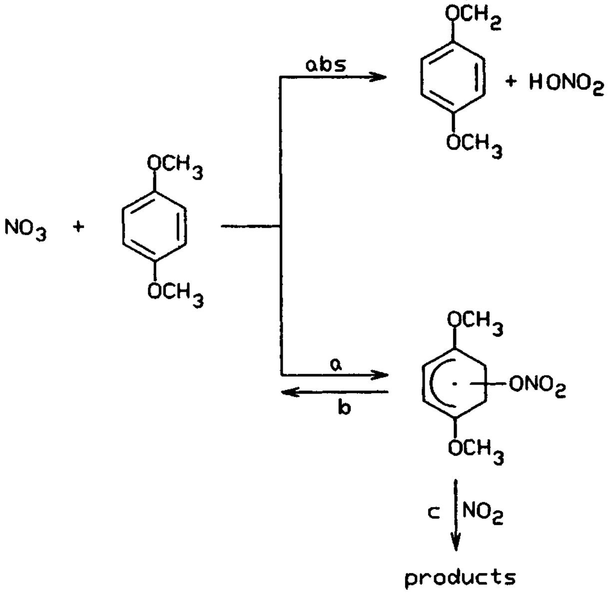

with the NO_3 radical addition reaction to the aromatic ring leading, in part, to nitrodimethoxybenzene formation.

The nitrodimethoxybenzene yields from the NO_3 radical addition reactions with the dimethoxybenzenes can be obtained by correcting the measured nitrodimethoxybenzene yields for the fraction of reaction proceeding by H-atom abstraction. Using the values of k_{abs} and $k_a k_c/k_b$ given in Table II and the measured nitrodimethoxybenzene yields given in Table III, then the yields from the NO_3 radical addition pathway are given by (nitrodimethoxybenzene yield from NO_3 radical addition) = (measured nitrodimethoxybenzene yield) × $\{k_{abs} + (k_a k_c[NO_2]/k_b)\}/(k_a k_c[NO_2]/k_b)$ and are given in Table III. The calculated nitrodimethoxybenzene yields from the NO_3 radical addition pathway exhibit a significant amount of scatter, in part due to the uncertainties in the values of k_{abs} and $k_a k_c/k_b$. Unit-weighted averages of the data given in Table III lead to nitrodimethoxybenzene yields from NO_3 radical addition to the aromatic rings of 0.50 for the formation of 4-nitro-1,2-dimethoxybenzene from 1,2-dimethoxybenzene, 0.42 for the formation of 4-nitro-1,3-dimethoxybenzene from 1,3-dimethoxybenzene, and 0.20 for the formation of 2-nitro-1,4-dimethoxybenzene from 1,4-dimethoxybenzene, all with estimated overall uncertainties of a factor of ca. 2. These nitro-product yields from the NO_3 addition reactions with the dimethoxybenzenes are of a similar magnitude to the nitrophenol yields from the NO_3 radical reactions with phenol and *o*-, *m*-, and *p*-cresol of 0.13–0.74 [19]. If it is assumed that the formation of nitrodimethoxybenzenes from the NO_3 radical reactions with the dimethoxybenzenes occurs by an analogous mechanism to that for the formation of nitro-aromatics from the OH radical reactions with benzene, toluene, and the xylenes in the presence of NO_x [23,24], then the formation of 3- and 4-nitro-1,2-dimethoxybenzene from 1,2-dimethoxybenzene, mainly 5-nitro-1,3-dimethoxybenzene from 1,3-dimethoxybenzene, and 2-nitro-1,4-dimethoxybenzene from 1,4-dimethoxybenzene would be expected [24]. The formation of only 4-nitro-1,3-dimethoxybenzene from the NO_3 radical reaction with 1,3-dimethoxybenzene is therefore not presently understood.

The kinetic data for the NO_3 radical reaction with dibenzo-*p*-dioxin are consistent with Reaction Scheme I and eq. (I), in that with no initially added NO_2 the rate of reaction of dibenzo-*p*-dioxin is close to zero, and increases with increasing NO_2 concentration. The experimental data indicate that for NO_2 concentrations $\geq 4.8 \times 10^{13}$ molecule cm^{-3}, back-decomposition of the NO_3-aromatic adduct to reactants [reaction (b)] cannot compete with reaction of the adduct with NO_2 [reaction (c)], and the measured rate constant is then k_a. Equation (I) can be rearranged in the form

$$\text{(IV)} \qquad \frac{1}{k_{obs}} = \frac{1}{k_a} + \frac{k_b}{k_a k_c [NO_2]}$$

and the rate constant k_a and rate constant ratio $k_a k_c / k_b$ can be obtained from a plot of k_{obs}^{-1} against $[NO_2]^{-1}$. The NO_2 concentrations during the N_2O_5-ethane-dibenzo-*p*-dioxin-air reactions were not measured since it is expected that chemiluminescence NO—NO_x analyzers also respond to N_2O_5. However, the NO_2 concentrations can be approximately estimated by assuming that every N_2O_5 molecule added to the chamber led to the production of an NO_2 molecule from the dissociation of N_2O_5. This was likely to be the case since the major loss process of NO_3 radicals in this reaction system was with 1-butene, which was present in 100-fold excess over dibenzo-*p*-dioxin.

$$N_2O_5 \xrightarrow{M} NO_2 + NO_3$$

$$NO_3 + \text{1-butene} \longrightarrow \text{products}$$

With this assumption and weighing heavily the values of k_{obs} obtained in the presence of initially-added NO_2 (Table I), then

$$k_a = 6.8 \times 10^{-14} \text{ cm}^3 \text{ molecule}^{-1} \text{ s}^{-1}$$

at 297 ± 2 K, with an estimated overall uncertainty of ±50%, and $k_a k_c / k_b = 3.9 \times 10^{-27}$ cm^6 $molecule^{-2}$ s^{-1}, with an estimated uncertainty of a factor of ca. 2. A plot of the rate constant ratio k_{obs} against the NO_2 concentration is shown in Figure 5, with the curve being given by the above values of k_a and $k_a k_c / k_b$. The agreement is reasonable, considering that the values of k_{obs} in the experiments without initially added NO_2 were derived from the slopes of the curved plots shown in Figure 1.

The formation of only 2-nitrodibenzo-*p*-dioxin suggests that the initial position of NO_3 radical addition to dibenzo-*p*-dioxin is either at the 1- position, followed by addition of NO_2 [reaction pathway (c)] at the 2-position with elimination of nitric acid, or at the 2- position followed by addition of NO_2 only at the 3- position, with

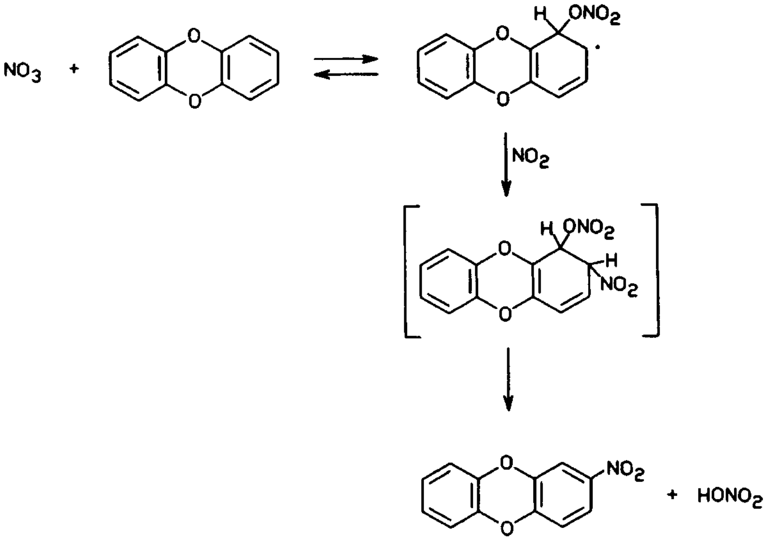

elimination of nitric acid leading to 2-nitrodibenzo-*p*-dioxin. However, the low yield of 2-nitrodibenzo-*p*-dioxin of 0.002 shows that other, as yet unidentified, products are dominant. This low yield of nitro-products from the NO_3 radical reaction with dibenzo-*p*-dioxin is in contrast with the fairly high yields of nitroarenes from the NO_3 radical-initiated reactions of naphthalene, 1- and 2-methylnaphthalene, acenaphthene (for addition to the aromatic rings) and fluoranthene of ca. 0.2–0.4, but is similar to the low yields of nitroarenes observed from the NO_3 radical reactions with phenanthrene, anthracene, and pyrene [2,4,9,11,25].

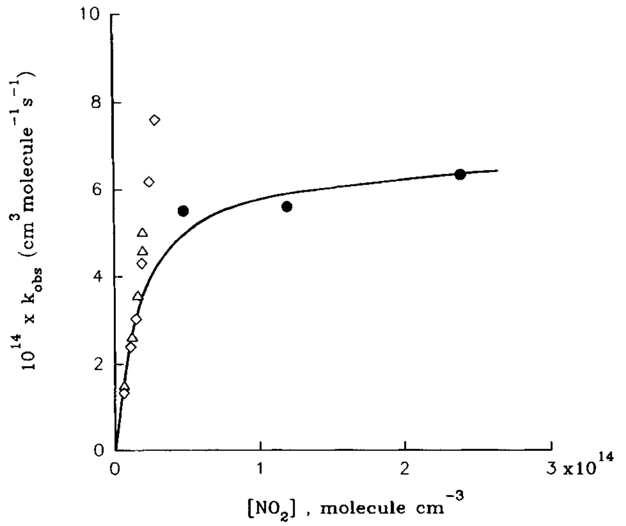

Figure 5. Plot of the values of k_{obs} against the NO_2 concentration for the reaction of dibenzo-*p*-dioxin. (●) from experiments with initially-added NO_2 (Table I); (△, ◇) from experiments with no initially added NO_2, with the NO_2 concentrations being estimated from the amounts of N_2O_5 added to the chamber (see text); and (—) calculated from eq. (I) with $k_a = 6.8 \times 10^{-14}$ cm^3 molecule^{-1} s^{-1} and $k_a k_c / k_b = 3.9 \times 10^{-27}$ cm^6 molecule^{-2} s^{-1} (see text).

TABLE IV. Rate constant ratios $k_a k_c/k_b$ and k_b/k_a and estimated rate constants k_a and k_b at room temperature for the reactions of the NO_3 radical with selected aromatic compounds.

Aromatic	$k_a k_c/k_b$ (cm^6 $molecule^{-2}$ s^{-1})	k_b/k_a[b] (molecule cm^{-3})	k_a[c] (cm^3 $molecule^{-1}$ s^{-1})	k_b (s^{-1})
Biphenyl[a]	$<5 \times 10^{-30}$	$>6 \times 10^{18}$		
Naphthalene[a]	3.6×10^{-28}	8.3×10^{16}	$>1.2 \times 10^{-13}$	
1-Methylnaphthalene[a]	7.7×10^{-28}	3.9×10^{16}	$>6 \times 10^{-13}$	
2-Methylnaphthalene[a]	1.08×10^{-27}	2.8×10^{16}	$>5 \times 10^{-13}$	
2,3-Dimethylnaphthalene[a]	1.55×10^{-27}	1.9×10^{16}	$>7 \times 10^{-13}$	
Acenaphthene[a]	1.65×10^{-27}	1.8×10^{16}	$>1.9 \times 10^{-12}$	
1,2-Dimethoxybenzene	1.0×10^{-28}	3.0×10^{17}	$>4 \times 10^{-14}$	
1,3-Dimethoxybenzene	3.3×10^{-29}	9.1×10^{17}	$>4 \times 10^{-14}$	
1,4-Dimethoxybenzene	1.3×10^{-28}	2.3×10^{17}	$>6 \times 10^{-14}$	
Methoxybenzene	$<7 \times 10^{-30}$	$>4 \times 10^{18}$		
Dibenzofuran	$<7 \times 10^{-30}$	$>4 \times 10^{18}$		
Dibenzo-*p*-dioxin	3.9×10^{-27}	7.7×10^{15}	6.8×10^{-14} [d]	520[d]
1-Nitronaphthalene[a]	3.0×10^{-29}	1.0×10^{18}	$>1.5 \times 10^{-14}$	
2-Nitronaphthalene[a]	2.7×10^{-29}	1.1×10^{18}	$>1.3 \times 10^{-14}$	

[a] From ref. [4].
[b] With $k_c = 3 \times 10^{-11}$ cm^3 $molecule^{-1}$ s^{-1} (see text).
[c] From ref. [1] and [18]; see text.
[d] This work.

The present kinetic data for the NO_3 radical reaction with dibenzo-*p*-dioxin provide important new insights into the reactions of the NO_3 radical with aromatic compounds. In particular, the rate constant for the addition of the NO_3 radical to dibenzo-*p*-dioxin (k_a) has been obtained. Previously, only values for the rate constant ratios $k_a k_c/k_b$ were available [4], and Table IV gives the present and literature values of the rate constant ratios $k_a k_c/k_b$. Apart from dibenzo-*p*-dioxin, none of the individual rate constants k_a, k_b, or k_c have been experimentally measured. However, Knispel et al. [26] have measured temperature-independent rate constants of $(2.4-4.0) \times 10^{-11}$ cm^3 $molecule^{-1}$ s^{-1} at 300–353 K for the analogous reactions of NO_2 with the hydroxycyclohexadienyl, methylhydroxycyclohexadienyl, and dihydroxycyclohexadienyl radicals formed from OH radical addition to benzene, toluene, and phenol, respectively. Assuming that the rate constant k_c for reaction of NO_2 with the NO_3-aromatic adduct is similar to those for the reactions of NO_2 with the OH-benzene, OH-toluene, and OH-phenol adducts, then use of $k_c = 3 \times 10^{-11}$ cm^3 $molecule^{-1}$ s^{-1} at 298 K leads to the values of k_b/k_a given in Table IV.

For dibenzo-*p*-dioxin, use of the measured rate constant $k_a = 6.8 \times 10^{-14}$ cm^3 $molecule^{-1}$ s^{-1} leads to the thermal decomposition rate constant k_b of

$$k_b = 520 \text{ s}^{-1} \quad \text{at } 297 \pm 2 \text{ K},$$

uncertain by at least a factor of 2. However, no data are available for the rate constants k_a for the other aromatic compounds for which rate constant ratios $k_a k_c/k_b$ have been measured, although lower limits to k_a are available from the data of Atkinson and Aschmann [1] and Atkinson et al. [18] for naphthalene, 1- and 2-methylnaphthalene, 2,3-dimethylnaphthalene, acenaphthene, and 1- and 2-nitronaphthalene, and these are also given in Table IV. Atkinson et al. [3,4] assumed for naphthalene that the

NO_3 radical addition rate constant k_a was similar to that for OH radical addition to naphthalene. However, the rate constant k_a for addition of the NO_3 radical to the aromatic rings of dibenzo-*p*-dioxin is a factor of ca. 200 lower than the rate constant for the corresponding OH radical reaction [13], indicating that the assumption of Atkinson et al. [3,4] was probably not valid. In fact, we have previously shown [19] that the rate constant for the gas-phase reaction of 2-nitrophenol with the NO_3 radical is a factor of >45 lower than that for the corresponding OH radical reaction, although it is not certain that the reaction pathways are the same for the NO_3 radical and OH radical reactions with 2-nitrophenol (and phenol and the cresols) [19].

Clearly, a knowledge of the rate constants k_a is needed before the NO_3-aromatic adduct thermal decomposition rate constants k_b can be derived. It should also be noted that the rate constants k_a and k_b may be in the fall-off regime, as is the case for the corresponding rate constants for the OH radical addition reaction to benzene at atmospheric pressure and below [12]. It is particularly interesting that reactions of the NO_3 radical by the addition channel are observed with the dimethoxybenzenes and dibenzo-*p*-dioxin, which have two —OR (R = alkyl or phenyl) substituent groups, while methoxybenzene and dibenzofuran, with one —OR substituent group, react via the addition channel only very slowly.

In addition to the NO_3-aromatic adducts reacting with NO_2 [reaction pathway (c)], reaction with O_2 may be expected by analogy with the hydroxycyclohexadienyl radicals [26].

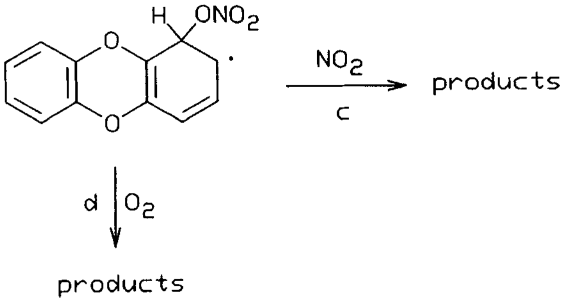

Any reaction of the NO_3-dibenzo-*p*-dioxin adduct with O_2, given by $k_a k_d[O_2]/k_b$, would appear as an intercept on the plot of k_{obs} against the NO_2 concentration and an upper limit is given as k_{abs} in Table II. From comparison of this value of $k_a k_d[O_2]/k_b < 8 \times 10^{-15}$ cm^3 molecule^{-1} s^{-1} ($k_a k_d/k_b < 1.6 \times 10^{-33}$ cm^6 molecule^{-2} s^{-1}) with that of $k_a k_c/k_b = 3.9 \times 10^{-27}$ cm^6 molecule^{-2} s^{-1} (Tables II and IV), then $k_d/k_c < 4 \times 10^{-7}$ at room temperature. With a rate constant of k_c ca. 3×10^{-11} cm^3 molecule^{-1} s^{-1} (see above), then $k_d < 1.2 \times 10^{-17}$ cm^3 molecule^{-1} s^{-1} at 297 K. This upper limit to the rate constant for reaction of the NO_3-dibenzo-*p*-dioxin adduct with O_2 is approximately an order of magnitude lower than the rate constants determined by Knispel et al. [26] of $(2-5) \times 10^{-16}$ cm^3 molecule^{-1} s^{-1} at room temperature for the reactions of O_2 with the hydroxycyclohexadienyl and methylhydroxycyclohexadienyl radicals formed from the OH radical reactions with benzene and toluene.

With the upper limit to the rate constant ratio k_d/k_c determined here, under atmospheric conditions the NO_3-dibenzo-*p*-dioxin adduct will react predominantly with NO_2 for NO_2 concentrations $\geq 2 \times 10^{12}$ molecule cm^{-3} (80 parts-per-billion mixing ratio). Since only an upper limit to k_d/k_c was obtained, the NO_2 reaction with the NO_3-dibenzo-*p*-dioxin adduct may be dominant at much lower NO_2 concentrations, such as those encountered in urban and maybe even rural areas.

Acknowledgment

The authors gratefully thank the U.S. Environmental Protection Agency, Office of Research and Development, for supporting this research through Assistance Agreement No. R-816198-01-0. Since the results described in this article have not been subjected to the Agency's review, no official endorsement should be inferred.

Bibliography

[1] R. Atkinson and S.M. Aschmann, *Int. J. Chem. Kinet.,* **20,** 513 (1988).
[2] J. Arey, B. Zielinska, R. Atkinson, and S.M. Aschmann, *Int. J. Chem. Kinet.,* **21,** 775 (1989).
[3] R. Atkinson, E.C. Tuazon, and J. Arey, *Int. J. Chem. Kinet.,* **22,** 1071 (1990).
[4] R. Atkinson, *J. Phys. Chem. Ref. Data,* **20,** 459 (1991).
[5] B. Rindone, F. Cariati, G. Restelli, and J. Hjorth, *Fresenius J. Anal. Chem.,* **339,** 673 (1991).
[6] E.C. Tuazon, J. Arey, R. Atkinson, and S.M. Aschmann, *Environ. Sci. Technol.,* **27,** 1832 (1993).
[7] R. Atkinson, *J. Phys. Chem. Ref. Data,* **Monograph 2,** 1 (1994).
[8] J.N. Pitts, Jr., R. Atkinson, J.A. Sweetman, and B. Zielinska, *Atmos. Environ.,* **19,** 701 (1985).
[9] R. Atkinson, J. Arey, B. Zielinska, and S.M. Aschmann, *Environ. Sci. Technol.,* **21,** 1014 (1987).
[10] R. Atkinson and S.M. Aschmann, *Atmos. Environ.,* **21,** 2323 (1987).
[11] R. Atkinson, J. Arey, B. Zielinska, and S.M. Aschmann, *Int. J. Chem. Kinet.,* **22,** 999 (1990).
[12] R. Atkinson, *J. Phys. Chem. Ref. Data,* **Monograph 1,** 1 (1989).
[13] E.S.C. Kwok, J. Arey, and R. Atkinson, *Environ. Sci. Technol.,* in press.
[14] R. Atkinson, C.N. Plum, W.P.L. Carter, A.M. Winer, and J.N. Pitts, Jr., *J. Phys. Chem.,* **88,** 1210 (1984).
[15] R. Atkinson, S.M. Aschmann, and J.N. Pitts, Jr., *J. Phys. Chem.,* **92,** 3454 (1988).
[16] B.F. Rodorf, *Chemosphere,* **18,** 783 (1989).
[17] G. Saint-Ruf and B. Lobert, *Bull. Soc. Chim. France,* **1/2,** 183 (1974).
[18] R. Atkinson, S.M. Aschmann, J. Arey, B. Zielinska, and D. Schuetzle, *Atmos. Environ.,* **23,** 2679 (1989).
[19] R. Atkinson, S.M. Aschmann, and J. Arey, *Environ. Sci. Technol.,* **26,** 1397 (1992).
[20] T. Boublik, V. Fried, and E. Hála, *The Vapour Pressures of Pure Substances,* Elsevier, Amsterdam, The Netherlands, 1984.
[21] W.P.L. Carter, A.M. Winer, and J.N. Pitts, Jr., *Environ. Sci. Technol.,* **15,** 829 (1981).
[22] R. Atkinson, W.P.L. Carter, C.N. Plum, A.M. Winer, and J.N. Pitts, Jr., *Int. J. Chem. Kinet.,* **16,** 887 (1984).
[23] R. Atkinson, S.M. Aschmann, J. Arey, and W.P.L. Carter, *Int. J. Chem. Kinet.,* **21,** 801 (1989).
[24] R. Atkinson, S.M. Aschmann, and J. Arey, *Int. J. Chem. Kinet.,* **23,** 77 (1991).
[25] B. Zielinska, J. Arey, R. Atkinson, and P.A. McElroy, *Environ. Sci. Technol.,* **23,** 723 (1989).
[26] R. Knispel, R. Koch, M. Siese, and C. Zetzsch, *Ber. Bunsenges. Phys. Chem.,* **94,** 1375 (1990).

Received July 16, 1993
Accepted November 2, 1993